Journal of Contemporary Issues in Business and Government Vol. 25, No. 01, 2019
https://cibgp.com/

P-ISSN: 2204-1990; E-ISSN: 1323-6903
DOI: 10.47750/cibg.2019.25.01.034

Micro-scale horizontal-axis wind turbines get new air foil

P.NAVEEN REDDY 1, POLAMURI RAMA MOHAN REDDY 2,
ASSOCIATE PROFESSOR 2, ASSISTANT PROFESSOR 1,
Mail ID:naveena0346@gmail.com, Mail ID:polamurirammohanreddy@gmail.com,
Dept.: Mechanical
Pallavi Engineering College,
Kuntloor(V),Hayathnagar(M),Hyderabad,R.R.Dist.-501505.

ABSTRACT

The purpose of this research was to find the optimum dimensions for the blades of tiny, horizontal-axis wind turbines operating at low wind speeds. The blades were designed with efficiency in mind using the blade element momentum (BEM) theory of blade optimization. Single (W1 & W2) and multistage (W3) rotors with radii of 0.2 m, 0.4 m, and 0.6 m, and a variety of blade geometries, were studied. The BEM theory was implemented using MATLAB and XFoil to design a series of six innovative air foils (NAF-Series) for low Reynolds number applications on tiny horizontal axis wind turbines. In order to create the experimental blades, a 3D printer was used to create a virtual model of the blade. XFoil software was used to study the performance of recently developed air foils at Reynolds numbers of 100,000, including the NAF3929, NAF4420, NAF4423, NAF4923, NAF4924, and NAF5024. Tip speed ratios between 3 and 10 and angles of attack between 2 and 20 were examined. The power coefficient, lift coefficient, drag coefficient, and lift-to-drag ratio were optimized and studied by varying these parameters in MATLAB and XFoil software. Both the single- and multi-stage rotors had a cut-in wind velocity of around 3 meters per second. The optimum values for the ratio of tip speed to axial displacement were 0.08m, and the angle of attack was 6 degrees. At low Reynolds numbers, the proposed NAF-Series air foil blades outperformed the basic SG6043 and NACA4415 air foil designs in terms of aerodynamic performance and maximum output power.

Keywords:

Synonyms: blade geometry; 3D printer; power coefficient; solidity; tip speed ratio.

INTRODUCTION

Having reliable access to energy is crucial to building a prosperous economy and thriving society. Wind turbines use the power of the wind to create electricity, making them a sustainable energy source. Using an improved blade, the compact horizontal-axis wind turbine only needs a wind speed of 4.2 m/s to start up, making it suitable for use in roadside or rooftop installations without the need for further mechanical assistance (Lee et al., 2016; Ismail et al., 2018; & Abrar et al., 2014). Power for generating torque was drawn mostly from the turbine blade's leading edge (Wright and Wood, 2004; Clifton and Wood, 2007). For the blade design calculation of propeller performance, the Blade Element Momentum (BEM) model provides good accuracy and high computing efficiency. At about 6 meters per second of wind, the tested rotor reaches its maximum power coefficient value of 0.371, whereas the optimized rotor reaches its maximum value of 0.388. (Gur and Rosen, 2008; Hassan Zadeh et al., 2016). Three turbulence models were examined using computational fluid dynamics (CFD) and blade element momentum (BEM). Two-kilowatt (kW) compact horizontal axis wind turbines with 1.8-meter rotor radii and 6-to-1 tip speed ratios (TSRs) at low wind speeds were studied for use in rural settings (Chaudhary and Prakash, 2019; Suresh and Rajkumar, 2019). A dual-rotor turbine configuration was suggested and studied by Rosenberg et al., 2014. In this dual-rotor design, a smaller, aerodynamically optimized secondary coaxial rotor is positioned in front of the primary rotor. At the same tip speed ratio, the multistage wind turbine researched by Nugroho et al., 2019 performs better than the single rotor, and their research indicates that a (X/D) axial distance ratio of 0.18 is optimal. One of the primary goals of long-term preparation is the achievement of sustainable development.

DESIGN PROCESS FOR AIRFOILS AND BLADES

Thickness to camber ratios provide the basis for air foil research and development. There are now a variety of Low-Re HAWT air foils that have been simulated and analysed using the XFoil to aid in the selection of air foil procedures. For the purpose of evaluating the aerodynamic performances of novel air foils, the SG6043 and NACA4415 air foils were chosen based on their prevalence in the relevant literature and the results of the Foil analysis. The NAF is the official abbreviation for the new air foil. The work presented here includes the development and optimization of air foils for use in the rotors of small horizontal-axis wind turbines, including the NAF3929, NAF4420, NAF4423, NAF4923, NAF4924, and NAF5024. The multirotor design researched by Jaya Priya et al. (2019) may be utilized to maximize energy production in confined spaces.

When creating rotor blades, air foil is a crucial factor to consider. Increasing the air foil's lift-to-drag ratio improves its power coefficient and torque output (Chaudhary and Roy, 2015; Singh and Ahmed, 2012). Aerodynamic properties of air

P-ISSN: 2204-1990; E-ISSN: 1323-6903
DOI: 10.47750/cibg.2019.25.01.034

foils were analysed using Foil software on the 251 panels shown in Fig. 1. Changes were also seen in the new air foil's geometry, namely in the thickness-chamber ratio and the leading-edge radius. Different permutations of the maximum lift coefficient and the lift-to-drag ratios were used to separately alter both the Reynolds number and the Nacrite. Six novel air foil shapes were tested and compared to current low Re air foils in terms of their aerodynamic performance. Both the SG6043 and NAF4923 air foils had a high CL/CD ratio, which is essential for optimizing power production. With a 10% maximum thickness, SG6043 might lead to stress concentrations in the area around the plant's roots. NAF4923, a newly designed air foil, had a maximum thickness of 12.80% and a maximum thickness position of 29.70%, as well as a maximum camber of 5.71% and a maximum camber position of 41.90% with respect to the chord length. Comparisons to the NACA4415 and the SG6043 reveal that the lift coefficients of the NAF series are higher. When compared to the SG6043 air foil, the new air foil's greatest CL/CD ratio was attained at an angle of attack = 5° to 6°. However, with a Reynolds number of 1 105, the NACA4415 air foil's maximum CL/CD ratio was achieved at an angle of around 7°. Each of the three blade designs, which have rotor radii of 0.2 m, 0.4 m, and 0.6 m with varying degrees of solidity,

Tab. 1 displays the results of those studies. Figure 2 depicts a rotor blade design, and Figure 3 depicts an air foil with the optimal axial spacing between two rotors. At a ratio of 0.18, axial distances are at their most ideal (Nugroho et al., 2019).

Table 1. Wind turbine blade specification.

Rotor type	Rotor radius (m)	Solidity	Airfoil
R1	0.2	0.1181	NAF4923
R2	0.4	0.1463	NAF4923
R3	0.6	0.0523	NAF4923

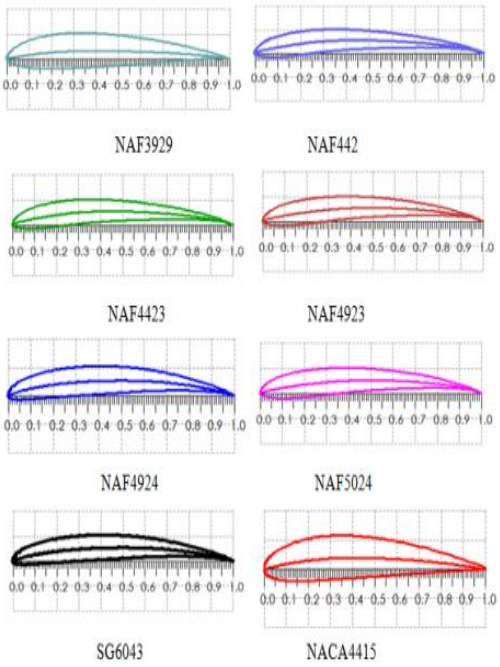

Figure 1. The following air foils may be made using the XFoil program: NAF3923, NAF4420, NAF4423, NAF4923, NAF4924, NAF5024, NACA4415, and SG6043.

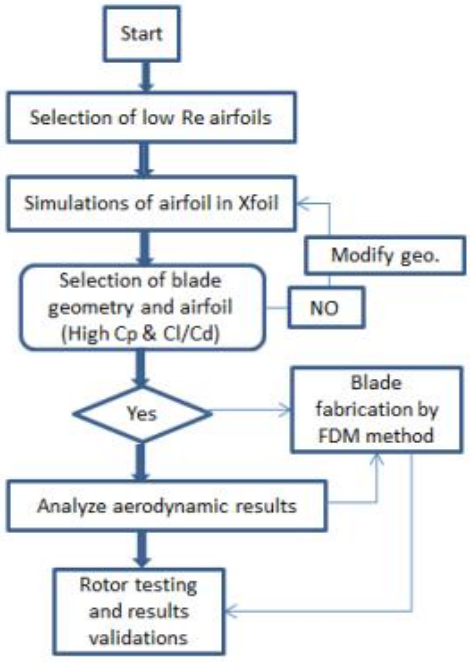

Figure 2. Flow chart of the methodology used air foil selection, blade design, and rotor testing.

P-ISSN: 2204-1990; E-ISSN: 1323-6903
DOI: 10.47750/cibg.2019.25.01.034

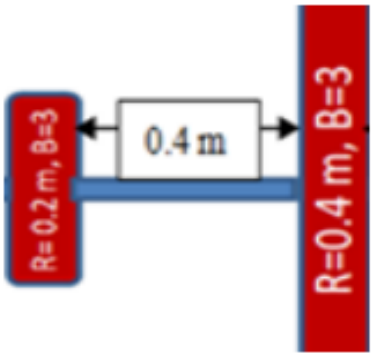

Figure 3. Rotor configuration.

PROCESSES OF MODELING AND ANALYSIS

Tab. 1 displays the results of experiments conducted to optimize and test three distinct blade pitch angles for a small wind turbine rotor blade made from ABS and PLA material using FDM. The blade has solidities of 11.81 percent, 14.63 percent, and 5.23 percent. Selecting a rotor's radius in relation to wind speed is shown graphically in Fig. 4 for a Reynolds number of 100,000. FIGURE 5 depicts the optimized blade shape of rotors R1, R2, and R3. For quick prototyping, Fig. 6 shows how the twist angle changes as the blade section length shifts for the redesigned air foil with B = 3. Models of XFoil and 3D-printed optimization blades' R1, R2, and R3 efficiencies are shown.

in Fig. 7. The R2 model's blades were made to be more solid, while the R3 model's blades were made to be less so. In order to examine rotor performance, XFoil was used. In Fig. 7, we saw the results of optimizing the FDM-fabricated 3D-printed W1 and W2. One-stage rotors were labelled W1 and W2. Rotor type W3 is, however, intended for use in multistage wind turbines. Tab. 2 shows the experimental rotor setup. Small wind turbines' aerodynamic performance may be determined with the use of this method [Ismail et al., 2018; Chaudhary and Roy, 2015].

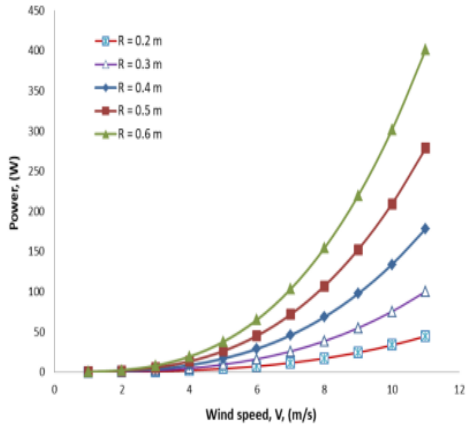

Figure 4. Selections of rotor radius.

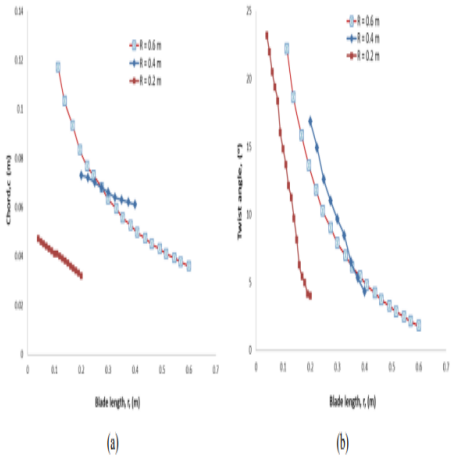

Figure 5. Optimum blade geometry of 0.2m, 0.4m, and 0.6m rotor radius. (a) Chord distribution along the blade length. (b) Blade twist distribution along the blade length.

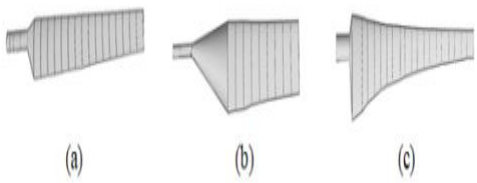

Figure 6. Optimum blade models: (a) R1, (b) R2, and (c) R3.

Table 2. Rotors configuration for experimentations'

P-ISSN: 2204-1990; E-ISSN: 1323-6903
DOI: 10.47750/cibg.2019.25.01.034

Blade types	Rotor types	Rotor radius (m)	Number of blades	Material
R1	W1	0.2	3	ABS
R2	W2	0.4	3	PLA
R1 & R2	W3	$R_f = 0.2$ & $R_r = 0.4$	6	ABS & PLA

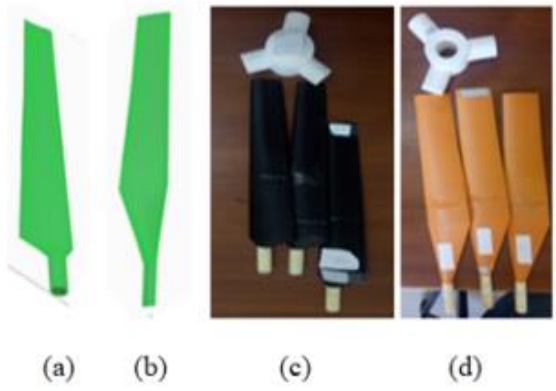

Figure 7. Shapes of blades in three dimensions (a-b) Blade models for R1 and R2 that were 3D printed and then optimized in the Cura program (c, d).

EXPERIMENTATIONS

Tab. 3 shows the various blade shapes and design parameters for small wind turbines. In Fig. 8, we saw the new air foil model that had been modelled in the Foil program. Figure 9 depicts the process of making the air foil model and rotor blade out of wood, printing ABS, and PLA filaments. Using the Cure program, the Creo files were converted to G code and then sent to the 3D printer. The printer was operated with the following parameters: nozzle temperature of 205°C, bed temperature of 60°C, and printing speed of 50 mm/s. Fig. 7 depicts the blade's construction with the new NAF4923 air foil. The fluid mechanics laboratory at the SPPU University-affiliated Dr. D. Y. Patil School of Engineering in India served as the experimental setting for the studies. Wind turbine blade test stands are shown in Fig. 10 (a, b) and Fig. 11 (a) throughout their production and experimentation phases. There is a 0.3 m 0.3 m 1 m test segment in the wind tunnel. Tabulated 4 displays detailed descriptions of mentioned technical instruments. Axial displacements of 0.04m, 0.06m, and 0.08m were used in the wind tunnel experiments, together with varying wind speeds, to calculate the rotor's output power (W3).

Table 3. Design parameters simulation details.

Parameters	Descriptions
Base airfoil selection	SG6043 & NACA4415
Angle of attack (α)	2° to 20°
Tip speed ratio (λ)	2 to 8
Solidity (σ)	0.0523 to 0.1463
New airfoil series	NAF
Reynolds No.	100000
Rotor radius	0.2 m, 0.4m, & 0.6m

Figure 8. Air foil model created in Xfoil.

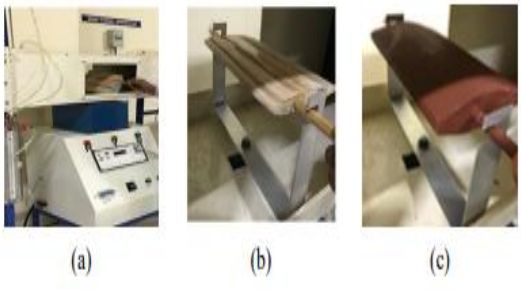

Figure 9. Experimental setup. (a) Controller unit, (b) 3D printer, and (c) wind tunnel.

Table 4. Test instrument details for experimentations.

Instrument	Model number	Measurement range	Resolutions	Temperature range
Anemometer	AVM-06	0.5–30 m/s	0.1 m/s	0 – 60 °C
Tachometer	HTM-560	10 to 1000 rpm	0.1 rpm	0 – 60 °C
Multimeter	AVF-19N	0.2 – 230 V	0.1 volt	0 – 60 °C
Wind tunnel	WT-02	1 -30 m/s	1 m/s	0 – 60 °C

The acceptable working temperature is between 0.075 and 0.3 m (or 0 and 60 °C). Two-rotor coaxial series wind turbines are taken into account in this study (b). The inverter battery system is shown in Fig. 12. When the wind speed drops, the second rotor's torque rises to match that of the first rotor, thus stopping the first rotor from spinning. Even at low wind speeds, the second rotor's mechanical output is boosted by the high torque.

P-ISSN: 2204-1990; E-ISSN: 1323-6903
DOI: 10.47750/cibg.2019.25.01.034

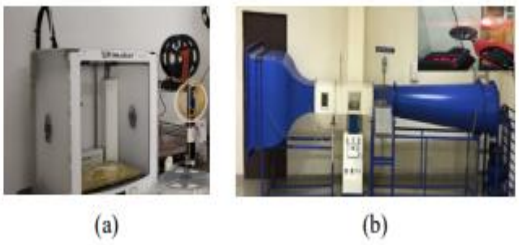

(a) (b)

Figure 10. Experimental setup. (a) 3D printer. (b) Wind tunnel.

(a) (b)

Figure 11. Schematic layout of the experimentations pictures: (a) W1, (b) W2, & W3

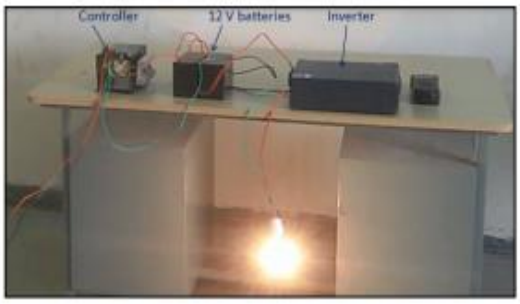

Figure 12. Inverter battery setup.

RESULTS AND DISCUSSIONS

This section presents the findings from the numerical and experimental studies conducted for all scenarios. Experiments were conducted on both single and multistage rotors, with rotor blade pitch angles ranging from 0 degrees to 90 degrees, and wind velocities ranging from the cut-in speed (2.5 to 3 m/s) to the rated wind speed (8 m/s). In Appendix A1, you'll find the MATLAB code for creating the blades (Appendix).

The Impact of Air foils on Rotor Efficiency

For low Reynolds number use in compact horizontal axis wind turbines, the NAF-Series air foil was evaluated alongside the SG6043 and NACA4415 base air foils. In order to develop and test the new air foils, XFoil was used with a Re value of 100000. By comparing and contrasting with other low-Reynolds-number air foils, XFoil software helped to optimize the AF300 (Singh et al., 2012). To meet all of the examined air foils' velocity requirements, the polar curves were calculated for values ranging from 0 to 20 degrees. Lift and lift-to-drag ratio graphs for the 8 airfoil at Re=100000 are shown in Figs. 13(a-b). The values of the lift coefficients are shown to be very sensitive to the angle of attack (a) in Fig. 13(a). Based on the data presented, the graph shows that the NAF-Series air foil achieves its maximum lift coefficient between 8 and 12 degrees of angle of attack. The graph shows that the NAF4420 and SG6043 air foils achieve their peak CL values of 1.65 and 1.66 at an angle of attack of 12o and 14o, respectively.

At an angle of 16 degrees, the NAF4924 air foil reaches its maximum CL of 1.5. Except for the NAF4924 air foil, the value of CL for NAF air foils drops after 12o angle of attack up to angle of attack, =16o, and after 16o angle of attack, the value of CL =1.35 - 1.5 stays constant up to 20o angle of attack. Maximum CL values of 1.35, 1.6, 1.5, 1.55, 1.5, 1.65, and 1.48 were achieved by the air foils NAF3929, NAF 4420, NAF4423, NAF4923, NAF4924, SG6043, and NACA4415 at an angle of attack, of 12o -16o, respectively. The NAF4923, NAF4924, and SG6043 air foils exhibited soft stall behaviour between 12 and 16 degrees of angle of attack. Except for NAF3929, the optimal lift-to-drag ratio for the new air foil was found at an angle of attack of 5°-6° and a Reynolds number of Re = 100,000. Maximum lift-to-drag ratios for the NAF3929, SG6043, and NACA4415 are at an angle of attack of 8 degrees, 7 degrees, and 10 degrees, respectively. Figures 13(a) and (b) show that at an angle of attack of 2o-10o, the NAF4923 air foil has a lift coefficient that is 10-15% greater than that of the SG6043 air foil due to its significant camber and thickness. When used to tiny power rotors, the high lift coefficient and its high AOA, at low speeds improved rotor start up and boosted its performance at low wind velocities. Figure 13(b) displays the CL/CD variance for several air foils at a Low Reynolds number =100,000. In order, the NAF4923 and NAF4924 air

P-ISSN: 2204-1990; E-ISSN: 1323-6903
DOI: 10.47750/cibg.2019.25.01.034

foils at = 6o and = 5o generated the highest lift-to-drag ratios (CL/CD) of 69, followed by the SG6043 and NACA4415 air foils at = 7o and = 10o, producing CL/CD = 66 and 48, respectively. Maximum CL/CD values for air foils NAF3929, NAF4420, NAF4423, and NAF5024 are 49, 66, 66.5, and 68 for = 8o, 5o, and 6o, respectively. At an angle of attack of 2o, the NAF4923 and SG6043 air foils had CL/CD ratios of 40 and 35, respectively, which were the lowest values found. According to the final tally of XFoil's findings, the NAF4923, NAF4924, and SG6043 air foils all produced their maximum lift-to-drag ratios at a single value, while the NAF5024 and NACA4415 air foils exhibited a soft stall behaviour in the angle of attack, between 2 degrees and 10 degrees. For low Reynolds number applications on small horizontal axis wind turbines, the NAF-Series air foil was shown to be the optimal profile.

At an angle of attack of 5–6 degrees and a Reynolds number of 100,000, the planned and optimized air foil showed its highest CL/CD ratio. To this end, we looked at how different rotor air foil sections affected the aerodynamic performance of our sample of tiny wind turbines. As compared to the SG6043 air foil, the suggested design had a thicker profile. The effect of air foil on the blade's efficiency is seen in Fig. 14. It is clear that NAF4923 and SG6043 achieve their maximum power coefficient at = 5. For ratios of 2 to 8, the BEMT-based design software was created. XFoil was used to generate the Cp- curve. Figure 14 shows the results of an analysis of the solidities of 5.23 percent with varied chord and twisted blade geometry at Re=100,000 for NAF4923 and SG6043 with and without root-tip losses for blade numbers, B=3. The highest power coefficient of the R3 blade model was 0.515 without root-tip losses and 0.46 with them, as shown in Fig. 14. The power coefficient of the SG6043 air foil decreases from its NAF4923 counterpart's values, but the value of rises from its starting point of 5. As a result, we'll be making and experimenting with blades based on the new air foil NAF4923. Figure 15 depicts the dynamic power output of the R1 rotor. 30 degrees is the ideal pitch angle for the blades of a rotor with an R1 rotor.

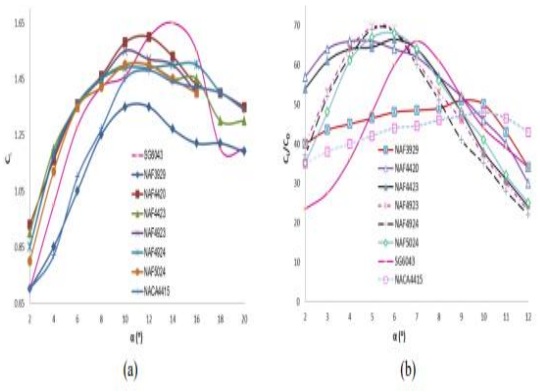

Figure 13. Variations of aerodynamic performances of different air foils: (a) CL vs α and (b) CL/CD vs α.

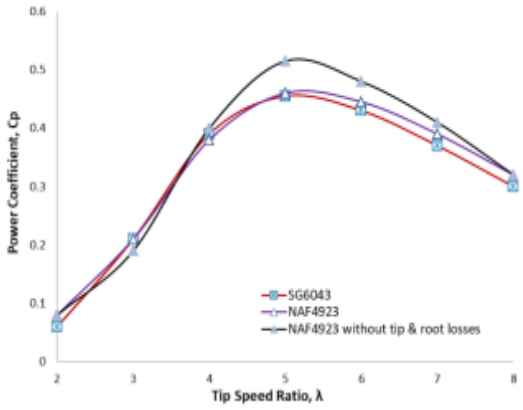

Figure 14. Variations of power coefficient of NAF4923 and SG6043 air foils of R3 blade model with and without blade root and tip losses.

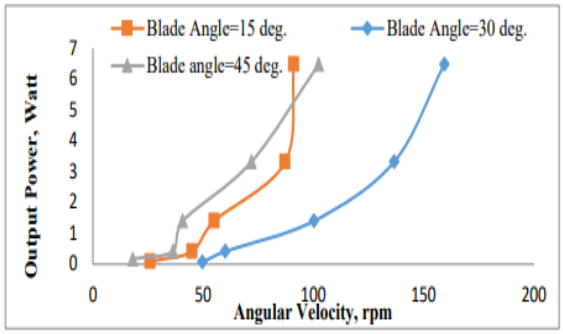

Figure 15. Variation of output power versus angular velocity of R1 rotor with optimum axial displacement of 0.08m at different blade pitch angles: (a) 15^{o} , (b) 30^{o} , and (c) 45^{o}.

ROTOR PERFORMANCE AS A FUNCTION OF SOLIDITY

P-ISSN: 2204-1990; E-ISSN: 1323-6903
DOI: 10.47750/cibg.2019.25.01.034

One of the most crucial factors influencing the efficiency of a horizontal axis wind turbine is its solidity (HAWT). FIGURE 16: The effect of rotor solidity on blade performances and tip speed ratios. For rotors R1 and R2 with solidity = 11.81% and 14.63%, respectively, the Cp values increase with a maximum tip speed ratio up to 4, and then decrease. In addition, the highest value of Cp for the R3 blade model was found to be at =5.5. The main effect is seen in Fig. 16 by comparing the solidity at different ratios of tip speeds. Tip speed ratios of 4, 4, and 5.5 yielded the highest Cp values of 0.36, 0.37, and 0.455, respectively.

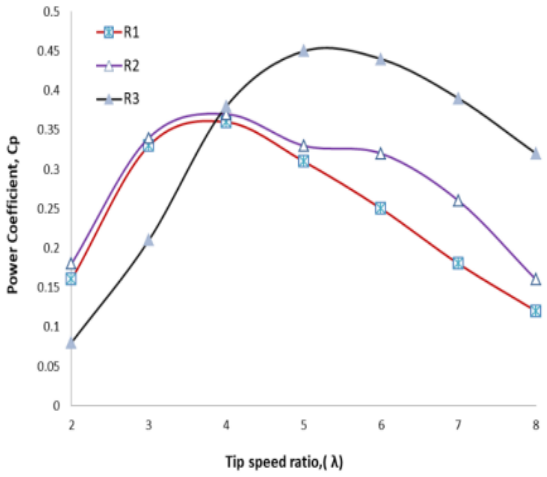

Figure 16. Power coefficient versus tip speed ratio at Re=100,000 for different rotors.

CONFIGURATION OF THE BLADE'S ANGLE OF PITCH AND THE ROTOR

The three different versions of wind turbines were put through their paces in a wind tunnel, where they were subjected to tests at varying blade pitch angles (from 0 degrees to 90 degrees, in 15-degree increments). At 0 and 90 degrees of blade pitch, the rotational speeds were both zero. Tab. 2 lists the rotors' technical specs. Experiments showing the performance of a rotor with three blades at optimal pitch angles of 15, 30, and 45 degrees for single and multistage rotors are shown in Figures 17 (a-c). Power production varies as a function of wind speed and optimal blade pitch angle, as seen in Figure 17. Blade pitch angle optimizations were performed on the W1, W2, and W3 models.

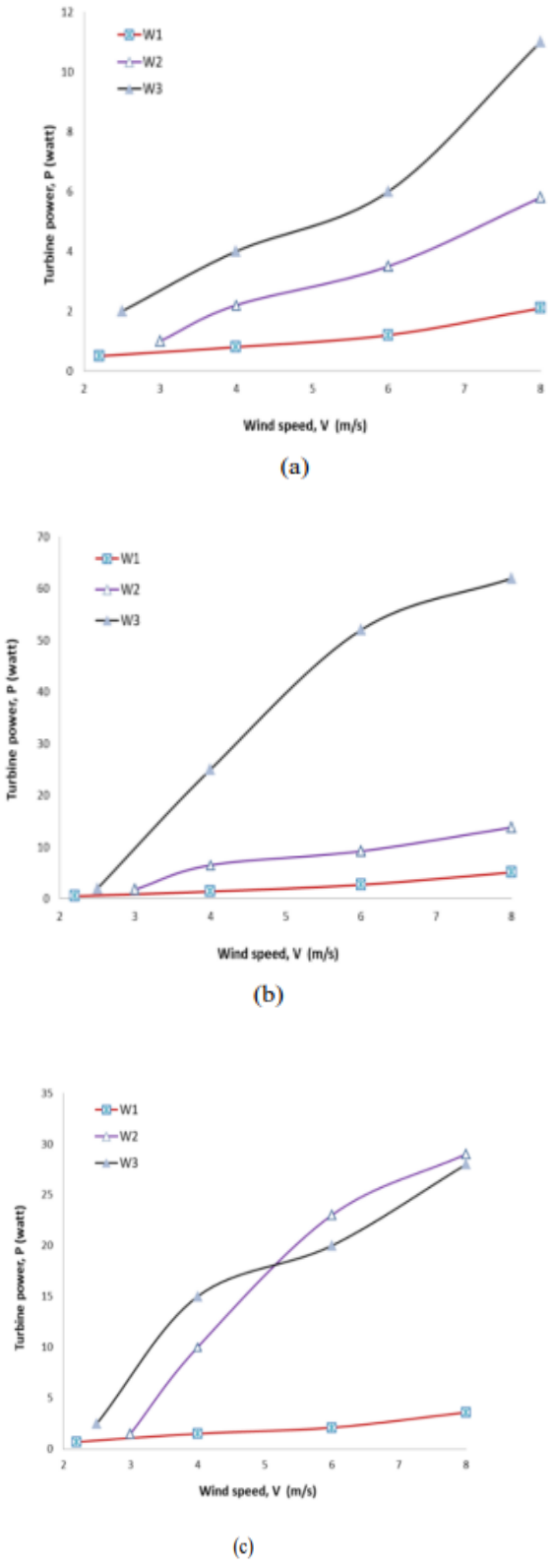

Figure 17. Power output of the different rotors at different wind speeds and blade pitch angles (a) 15°

P-ISSN: 2204-1990; E-ISSN: 1323-6903
DOI: 10.47750/cibg.2019.25.01.034

, (b) 30^o , and (c) 45^o . When compared to the W1 and W2 rotors, the proposed air foil NAF4923 and the W3 rotor performed the best. Since rapid prototyping can produce blades for specific needs without the need for expensive melds, it has great potential in the manufacture of small blades. For a W1 rotor, the initial wind speed was 2 m/s. The W2 and W3 models, on the other hand, had a minimum wind speed of about 2.5 m/s before they kicked in. Rotor W1, W2, and W3 of the wind turbine were optimized with a blade pitch angle of 30 degrees, 45 degrees, and 30 degrees, respectively. When the two rotors are displaced in opposite directions along their axes, the resulting mechanical power is altered. The value of the wind speed that will hit the second rotor varies depending on the axial displacement of the two rotors. In this study, we chose an axial displacement ratio of 0.08 m between the two rotors of the W3 model. To achieve maximum efficiency, the front (Rf) and rear (Rr) rotors' blade pitch angles should be set at 30 and 45 degrees, respectively. The graph depicts the maximum power output of a multistage wind turbine model (W3), with a blade pitch angle of 30 degrees. The rotors in the W3 model's wind turbine had front and back radii of 0.2 meters and 0.4 meters, respectively.

For a rated wind speed of 8 m/s, the rotor W1 generates mechanical power equal to 2.1 W at a blade pitch angle of 15o, 5.8 W at a pitch angle of 30o, and 11 W at a pitch angle of 45o. In addition, the rotor W2 generates mechanical power equal to 5.1 W, 13.8 W, and 62 W. Just like rotor W2, rated wind speed = 8 m/s generates mechanical power = 3.6 W, 62 W, and 28 W, respectively, at blade pitch angles of 15o, 30o, and 45o for rotor W3.

CONCLUSION

In this study, six newly-designed air foils (NAF-Series) were created and evaluated in XFoil at low Reynolds number. Compared to the SG6043 air foil, the numerical and experimental results suggested that the NAF4923 air foil was the most suitable for achieving the maximum power coefficient. In order to compare the CL, CL/CD, and SG6043 and NACA4415 air foils, six new air foils were measured and analysed. When developing small horizontal axis wind turbine rotors for low wind speed applications, the NAF-Series air foil and blade geometry optimization is an excellent choice. With an angle of attack () between 12 and 16 degrees and a Reynolds number (Re) of 100,000, the maximum CL for air foils NAF3929, NAF4420, NAF4423, NAF4923, NAF4924, SG6043, and NACA4415 was 1.35, 1.6, 1.5, 1.55, 1.5, 1.5, 1.65, and 1.48, respectively. Maximum CL/CD values of 49, 66, 66.5, 68, 69, 66, and 48 were achieved by air foils NAF3929, NAF 4420, NAF4423, NAF4923, NAF4924, SG6043, and NACA4415 at = 8o, 5o, 6o, 6o, 7o, and 10o, respectively, with Re=100,000. The NAF4923 and SG6043 had their blade geometries improved using BEMT in MATLAB and Foil. Using Xfoil, we optimized and studied rotor solidity at variable chord and twisted blade geometries with values of 11.81%, 14.63%, and 5.23%. Cp maxima of 0.36, 0.37, and 0.455 were achieved for blade types R1, R2, and R3 at values of 4, 4, and 5.5, respectively.

Using the FDM technique, we were able to quickly and cheaply produce three rotors based on the NAF4923 air foil section. The three wind turbine models (W1, W2, and W3) were tested at different wind speeds, axial displacement, and blade pitch angles. From Cp-λ performance, W3 with axial distance between two rotors was 0.08 m, being capable of producing better performance as compared to rotors W1 and W2 at the rated wind speed of 8 m/s. The maximum multistage wind turbine (W3) performances at axial displacement of 0.08m. The NAF-Series air foil is likely to be adopted for single and multistage horizontal axis wind turbines at low Reynolds number. The maximum power is produced by the rotor with solidity of 5.23 % at top speed ratio of 5.5. The optimum blade pitch angles = 30^o , 45^o , and 3^{0o} for W1, W2, and W3 rotors, respectively. The maximum mechanical power was achieved by W3 rotor. It can be said that W3 type of multistage wind turbine can be utilized for electricity generations.

REFERENCES

[1] Abrar, M. A., Mahbub, A. M. & Mamun, M. 2014. Design Optimization of a Horizontal Axis Micro Wind Turbine through Development of CFD Model and Experimentation,10th International Conference on Mechanical Engineering Procedia, Engineering, 90: 333-338.

[2] Chaudhary, M. K. & Roy, A. 2015. Design & optimization of a small wind turbine blade for operation at low wind speed, World journal of Engineering. 12 (1); 83-94.

[3] Clifton-Smith, M.J. & Wood, D. H. 2007. Further dual-purpose evolutionary optimization of small wind turbine blades, J. Phys. Conf. Ser., 75: 012017

[4] Chaudhary, M. K. & Prakash, S. 2019. Investigation of Blade Geometry and Air foil for Small Wind Turbine Blade Advanced Science, Engg and Medicine. 11 (5): 448-452.

[5] Duquette, M.M. & Visser, K. D. 2003. Numerical Implication of Solidity and Blade Number on Rotor Performance of Horizontal-Axis Wind Turbines, Journal of Solar Energy Engineering.125 (4):425-432.

P-ISSN: 2204-1990; E-ISSN: 1323-6903
DOI: 10.47750/cibg.2019.25.01.034

[6] Gur, O. & Rosen, A. 2008. Comparison between blade-element models of propellers. Aeronaut J.112:689–704.

[7] Hassan Zadeh, A., Hassan Abad, H.H. &Dad and, A. 2016. Aerodynamic shape optimization and analysis of small wind turbine blades employing the Veteran approach for post-stall region, Alexandria Engineering Journal. 55 (3): 2035-2043.

[8] Ismail, A.R.K., Thiago, Canali. & Fatima, A.M. Lino. 2018. Parametric analysis of Jankowskiair foil for10-kW horizontal axis windmill, Journal of the Brazilian Society of Mech. Sciences and Engineering. 40, Article no: 179.

[9] Jaya Priya, J., Muruganandam, D., Rajaraman, D., Senthil Kumar, B., and Dinakaran, V. 2019. Design and Fabrication of Multi-Rotor Horizontal Axis Wind Turbine" International Journal of Engineering and Advanced Technology (IJEAT), 8(6):3500-3504.

[10] Lee, M.H., Shiah, Y.C. & Chi Jeng, B. 2016. Experiments and numerical simulations of the rotor- blade performance for a small-scale horizontal axis wind turbine, J. Wind Eng. Ind. Aerodynamics.149: 17 – 29.

[11] Nugroho, S., Diana, L. & Ariyanti, D. P. 2019. Multistage Wind Turbine Capability to the Rotor Axial Distance Changes, International Electronics Symposium (IES), Surabaya, Indonesia, 359-363. Poole, S. & Phillips, R. 2015.

[12] Rapid Prototyping of Small Wind Turbine Blades Using 17 Additive Manufacturing, IEEE: South Africa. Rosenberg, A., Selvaraj, S. & Sharma, A. 2014. A novel dual-rotor turbine for increased wind energy capture. Journal of Physics (TORQUE 2014), 524:012078.

[13] Suresh, A. &Rajkumar, S. 2019. Design of small horizontal axis wind turbine for low wind speed rural application, Material today proceeding.23 (1):16-22.

[14] Singh, R.K. & Ahamed, M.R. 2013. Blade Design and Performance Testing of a Small Wind Turbine Rotor for Low Wind Speed Application, Renewable Energy. 50:812-819.

[15] Singh, R.K., Ahmed, M.R., Zillah, M.A., & Lee, Y.H. 2012. Design of a low Reynolds number air foil for small horizontal axis wind turbines, Renewable Energy.42:66–76.

[16] Wright, A.K. & Wood, D.H. 2004. The starting and low wind speed behaviour of a small horizontal axis wind turbine, Journal of Wind Engineering and Industrial Aerodynamics. 92:1265-1279.